Plumbing the Pudding Model of the Atom

By Eric Stanley Reiter, October 26, 2026, Pacifica, CA. http://www.unquantum.org

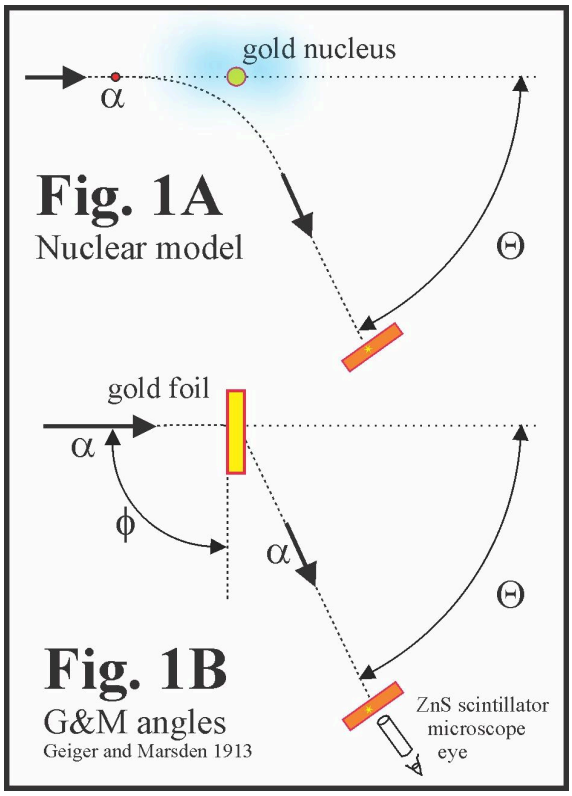


Fig. 1A
Nuclear model

Fig. 1B
G&M angles
Geiger and Marsden 1913

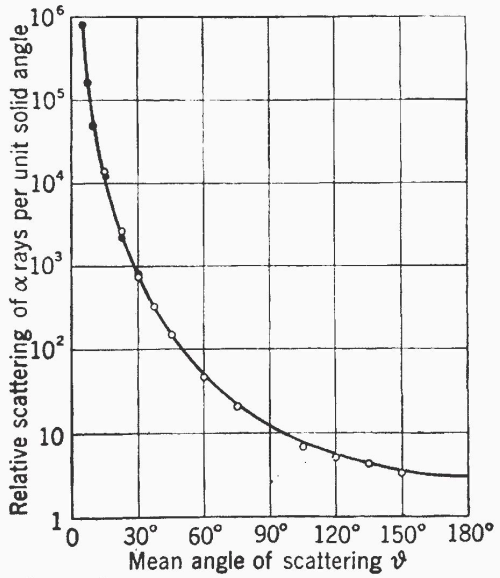


Fig. 2 α scatter from gold foil.
Data from Geiger and Marsden 1913.
Plot from Evans, *The Atomic Nucleus*, page 18.

Overview

We will explore in this sequence: **1)** the 1913 experimental evidence initiating the nuclear model, **2)** ER's (author) experimental repeat, **3)** theory of threshold model vs quantization, **4)** ER's past experiments with gamma γ and alpha α rays, **5)** ER's recent tests splitting the α upon a crystal surface, and **6)** conclusion. Beyond a serious challenge to quantization, this report shows <u>how</u> so-called nucleons can diffract. We know of experiments that show what appears to be nucleon interference (1, 2). If you do not think this is a problem, please read up on the *measurement problem*. The short answer is: if it diffracts, it is a wave. We explain particle-like effects as thresholds.

1) Early evidence of the nuclear model

An old atomic model depicts a massive positive charge extending to the size of its negative electronic influence. It is affectionately called *plum pudding*, a model proposed (not named) by JJ Thomson (3).

Rutherford's theory (4) on the scattering of alpha *particles*, Geiger and Marsden's G&M 1913 data (5), and Bohr's use of the nuclear model (6), led physicists to accept that the atom <u>must</u> have a small, heavy, positively charged nucleus; see **Fig. 1**. The 1913 fit to Rutherford's Coulomb derivation, as in **Fig. 2**, seemed convincing, but there are problems, especially at large angles. In modern enactments (7), background counts at angles exceeding 30° will overwhelm the effect. G&M's source emitted two alpha α of different kinetic energies $\mathcal{E}$. The theory depends on $\mathcal{E}$, and they lacked detectors with pulse-height resolution. They seemingly overcame those problems by using an extremely strong source and a filter ahead of the gold scatterer that allowed only the swiftest α to interact with the gold and their zinc sulfide scintillation viewer.

In modern practice, pulse-height resolution and discriminator settings should play a major role. In our search, we have not found anyone reporting this test with pulse-height resolution, nor have we found anyone

substantiating Rutherford theory as a function of angle at large angles (7, 8). The data of **Fig. 2** is from a table in G&M (5) that reported no error analysis. The graph was not in (5). Was this graph in Evans (9), generated by Evans?

Fig. 1B shows how G&M oriented their scattering foil. The foil and source were connected, and the detection viewer rotated. Different angles would change the interaction cross-section, which they did not seem to account for. Given the problems mentioned, the accuracy of the G&M report led me to see what it takes to repeat their effect.

2) Repeating the 1913 Geiger Marsden Rutherford test

My previous tests using the coincidence technique had such a low α coincidence background rate that the singles rate background was not a problem. However, α background from the steel and welds of my vacuum chamber is a significant problem with this test. To reduce that background, I lined the chamber with plastic tape and plastic parts. This made some compromise to the vacuum, but it stabilized near 5 x 10^{-1} torr; no compromise to my short-range α spectroscopy.

The α source was a collection of ^{241}Am mounted behind a collimator made of 55 glass pipettes (see **Fig. 7**). The detector is an ORTEC DIAD surface barrier with a built-in amplifier, unfortunately no longer available. The amplifier and pulse height discriminator were the ORTEC 490B and 551, respectively. The scatterer was LA-brand triple-thick 24K gold leaf, stacked 20 times to 0.0003 cm thick. We calculated this by weighing it with its paper, cutting it up, and subtracting the paper weight.

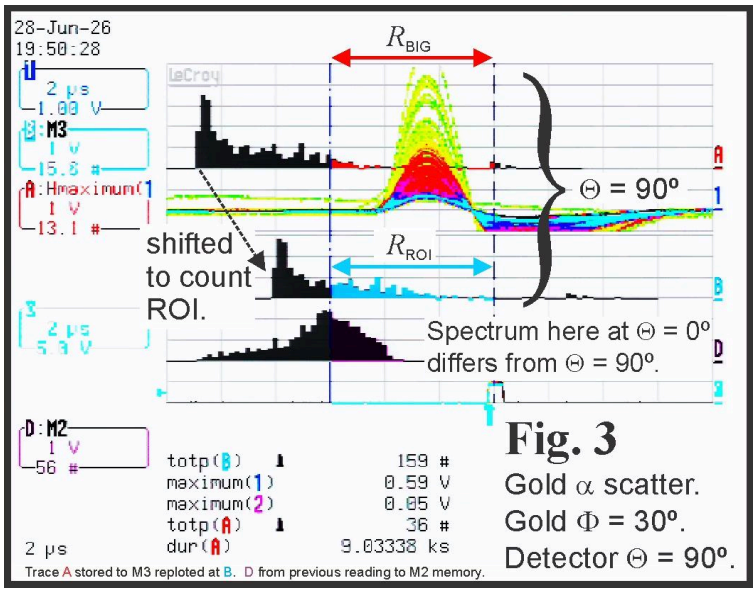


Fig. 3 Gold α scatter. Gold Φ = 30°. Detector Θ = 90°.

For each reported angle, data were collected on a Lecroy LT624 digital oscilloscope with histogram software. Data for scatterer angle Θ = 90° is shown in **Fig. 3**. Analog pulse heights are plotted in histogram A and copied, shifted to the right, onto trace B. We measure rates from the same test in two regions: at the BIGs region totp(A)/dur(A) = R_{BIG}, and at the ROI region totp(B)/dur(A) = R_{ROI}. In all cases, the angle of incidence of α to the gold was ϕ = 30°, where ϕ is defined in **Fig. 1B**.

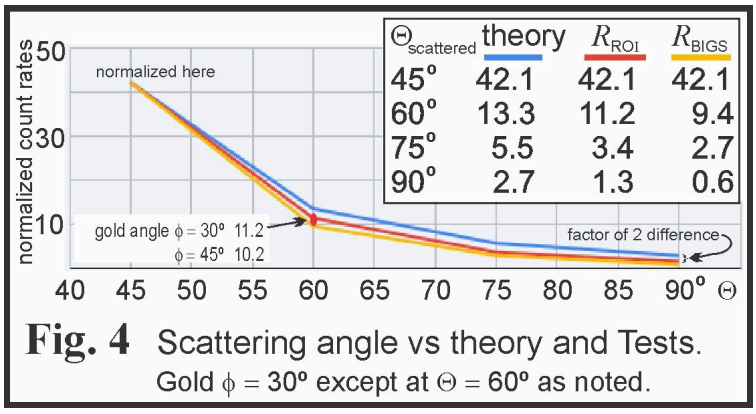


Fig. 4 Scattering angle vs theory and Tests. Gold ϕ = 30° except at Θ = 60° as noted.

Here, we see the importance of choosing which pulse heights to record as a function of detector angle Θ. Trace D shows pulse heights from a previous test through the gold at Θ = 0° to see how greatly the spectra change from 0° to 90°. The shape changed gradually with angle. A downshifted part of the spectrum lets more α pass at larger angles. The argument for choosing the count region is complicated, so we collected both rates and compared the results. An

interesting paper (10) deals with pulse heights, but it used only a low-level pulse-height discriminator, not a spectrum. Their data stopped at 75°.

Fig. 4 compares my data with theory. **Appendix 1** is a GOOGLE SHEETS spreadsheet that outlines all the steps. A link is provided for anyone to work with my original data. Using counts in my ROI, the data at Θ = 90° drifts from theory by a factor of 2. Given my weak source, wide ΔΘ angle (see **Fig. 7**), and other possible inaccuracies, we call this good. *Melissinose's* (7) error bar for data at 30° was a factor of 3 larger than theory.

An extension of Rutherford's theory is *Rutherford Backscattering Spectroscopy*. In my search, RBS is performed only at a large fixed angle. In my search, at large angles, Rutherford's equation is not obeyed at high energies. In my search, I found anomalies at large angles with some scatterers, interestingly reflecting from ^{128}Si at a similar MeV to ours (11). Evidently, large-angle conformation to the Rutherford equation is difficult to achieve. I am puzzled by how G&M achieved such accurate-looking data. Rutherford's original argument, and that of most physicists, emphasizes that α can scatter, and, more importantly, reflect backward, only with a particle model. In section **4** we show evidence that Bragg scattering can explain reflection.

3) ER's Theory in Brief

My previous work (12) explains how historical tests were not designed to distinguish quantization from a workable threshold model. False assumptions led people to eliminate what was called the loading theory (an unworkable threshold model). The historical tests we have treated include: the element of time in the photoelectric effect, the Bothe-Geiger experiment, the Compton-Simon experiment, the photoelectric effect, the blackbody spectrum, oil drop measurement of *e*, and all previous beam-split coincidence tests of the photon model.

A Quantum Mechanical QM particle, like a nucleon, is generally understood to go one way or another at a beam splitter. We perform beam-split coincidence tests with γ and α-rays, and see coincidence rates R_e far exceeding chance R_c. We call $R_e/R_c > 1$ the unquantum effect. Exceeding unity reveals the flaw of QM and removes nonlocality. Our threshold model interprets our constants *h*, *e*, and *m* (Planck's constant, charge, and mass) as thresholds. Ratios of these constants, like h/m, remain quantized. A matter wave of conserved ratios can thin out, load up to a threshold at an absorber, and give the illusion that a particle crash-landed. The matter wave can hold together to appear like a particle, or lose that ability, like a soliton.

4) α-split tests with gold (13, 16, 17)

Fig. 5 shows two surface barrier detectors a cm apart. ^{241}Am, emitting one 5.5 MeV α per decay, was aimed from a side perch toward the right detector, which is covered with gold leaf. This geometry accepts the widest range of interaction angles. The Lecroy scope triggers upon clicks within a preset time window τ to record both pulse heights. The computer plots the pulse heights in an XY graph as shown. Most of the pulses are half height. We calculate a ratio exceeding chance, $R_{experiment}/R_{chance}$, where $R_{chance} = R_1R_2\tau$, and τ = 100 ns. Using the half-height pulses $R_{experiment}/R_{chance} = 100$. QM predicts chance (ratio = unity), and we call exceeding chance the unquantum effect. Counting the larger pulses exceeds chance by 4. We perform an energy budget based on the characteristic pulse height. When we add the pulse heights of the larger pulse pair, the sum exceeds the characteristic pulse height. The energy budget per pulse pair easily exceeds unity and chance. By a *non-quantized* understanding of *energy conservation*, pre-loaded energy can add to the incident matter wave. Upon impact, the matter reaches a threshold.

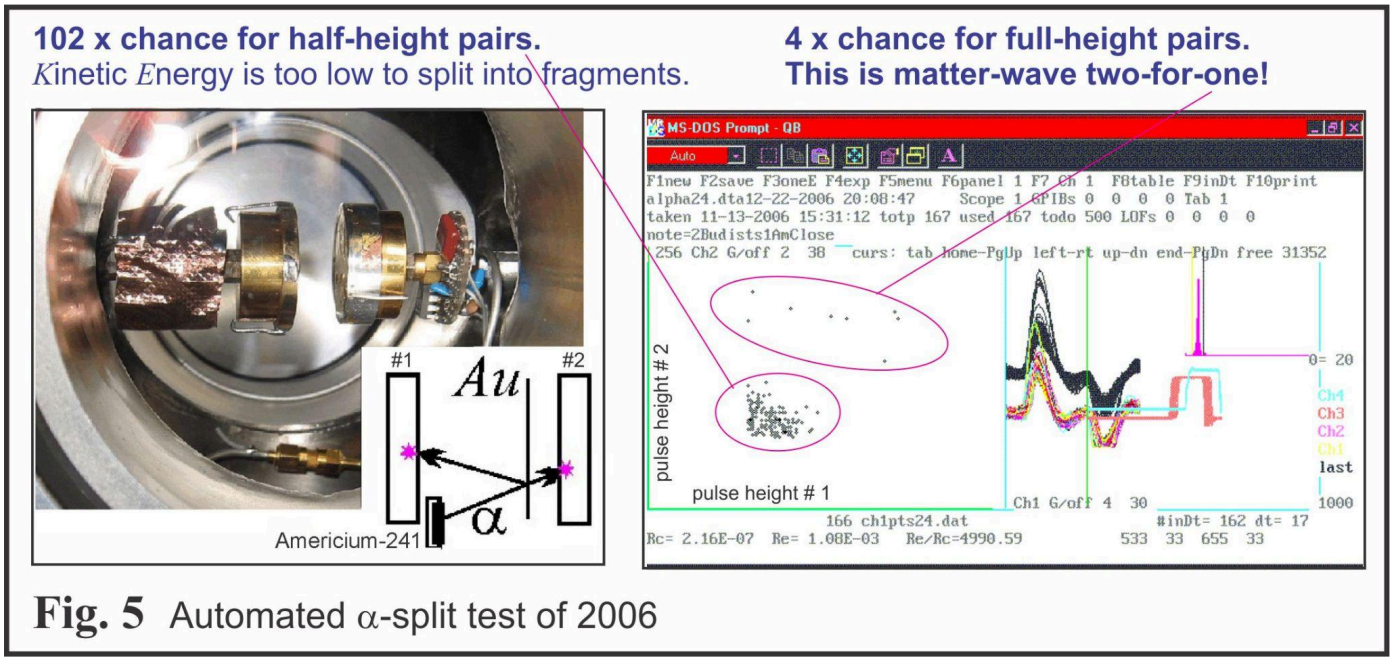


Fig. 5 Automated α-split test of 2006

When *threshold* is reached, it looks like a particle was absorbed. We are not splitting the α into two deuterons (which requires 14 MeV), nor are we breaking gold nuclei (which requires 26 MeV). We only have 5.5 MeV of kinetic energy. Our measured coincidence background was 1 count over 3 days. All pulses were perfect. A true coincidence test (test for one α emitted per spontaneous decay) revealed zero *trues*. Test of **Fig. 5** was from Nov 8-13, 2006. Recent tests have confirmed exceeding what we call *particle energy conservation* by a different method. We are splitting the matter wave.

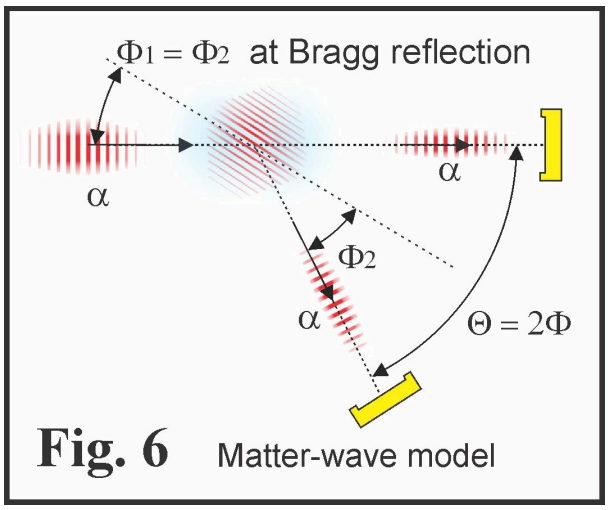


Fig. 6 Matter-wave model

5) New α-split tests

Fig. 6 outlines how to think about the matter-wave-to-matter-wave interaction we provide evidence for. Here, we use a crystalline scatterer, the silicon surface barrier detector. This detector serves a dual purpose: it detects and acts as the unquantum beam-splitter. My previous tests of this matter-wave unquantum effect used gold beam splitters (as above). We adjust the scatterer and deflection detector angles to test for specular reflection, characteristic of Bragg reflection. Coulomb repulsion theory does not predict specular reflection. Reports of Si crystal α-scattering (13) and specular reflection of atoms from crystals using the de Broglie equation support my model (14).

I performed 38 tests, keeping all variables unchanged except the angles of our two detectors. **Appendix 2** shows my complete spreadsheet. The detectors (see **Fig. 7**) are ORTEC surface-barrier type with built-in amplifiers, a discontinued model we were fortunate to find. The ^{241}Am α source is arranged behind the stack of 55 glass pipette tubes.

The crystal beam splitter enhanced the unquantum effect, but obviously, we are not dealing with atomic spacing. We calculate the matter wavelength as usual by: $\lambda = h/m_\alpha v$, and substitute v from kinetic energy $= \mathcal{E} = mv^2/2$, where $\mathcal{E} = 2*5.5\text{x}10^6\ eV$, and $m_\alpha = 3.7\text{x}10^9\ eV/c^2$. We obtain $\lambda = 6\text{x}10^{-15}$ m. Using Bragg

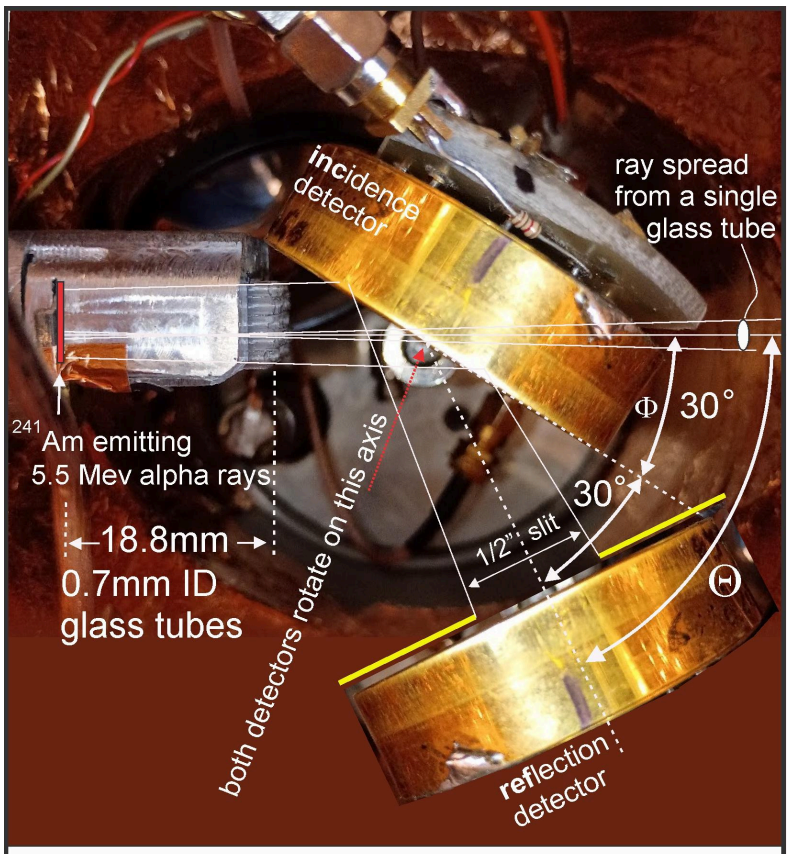


Fig. 7. Experiment at specular 30°.
The image of the reflection detector was pasted in.

diffraction at 30°, the distance between resonant reflective planes is 3×10^{-15} m. The distance between crystalline *Si* atoms is larger than the α matter-wavelength by 19.5 k. To review, the α splits in an *unquantum* sense in its interaction with nuclear-realm silicon. We are examining a matter-wave to matter-wave interaction.

The word "nuclear" distracts from this report's intent. We present evidence for an extended, massive, positively charged aspect of the atom with a periodic structure; not a tiny nucleus.

Fig. 8 shows selected screenshots from a Lecroy LT624 scope and a custom 4-channel MultiChannel Scaler MCS written in QUICKBASIC for this experiment. Except for angles read from external protractors, we obtained all data from these images. The LT624 triggers on timing edges from pulse-height discriminators (ORTEC 551) recorded on channels 3 and 4 that occur within a 2 μs window. Upon a trigger, the LT624 records the two timing edges, pulse

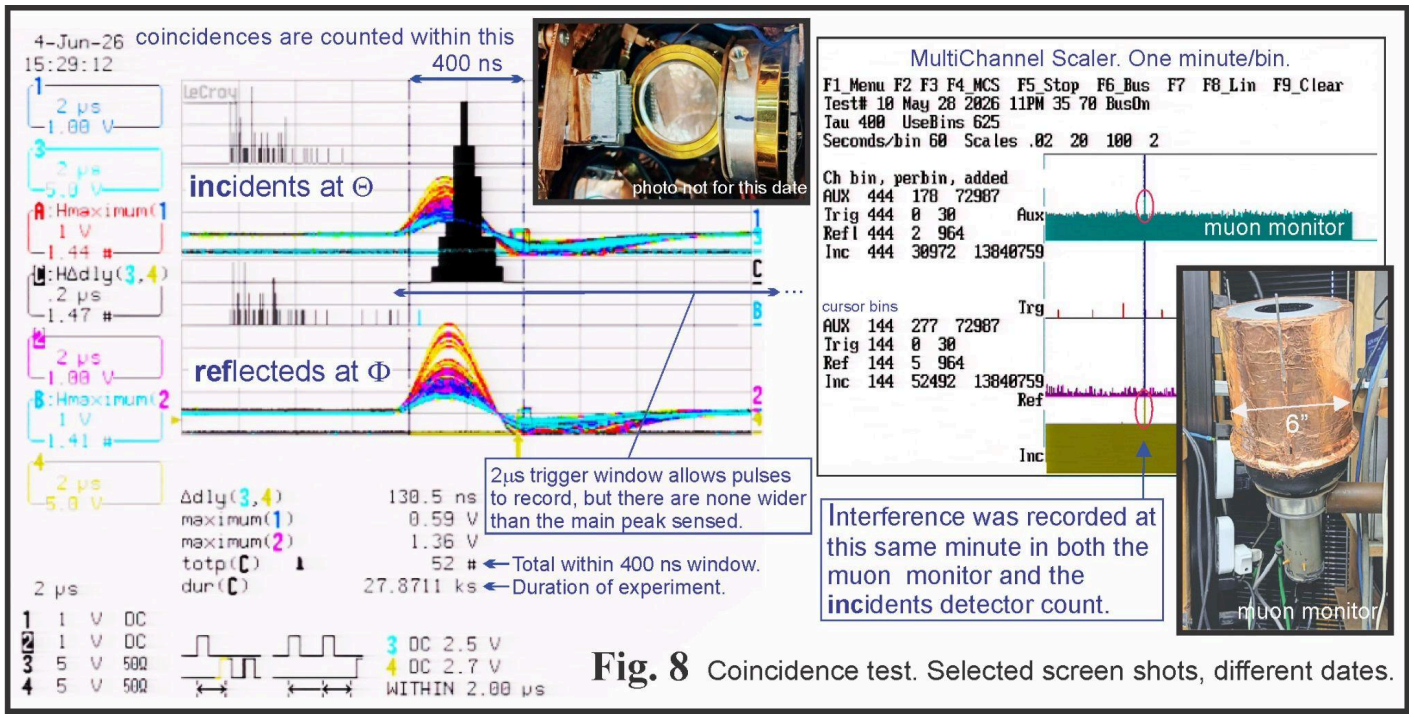


Fig. 8 Coincidence test. Selected screen shots, different dates.

shapes on traces 1 and 2, both pulse heights to histograms A and B, and histogram C of the time between those two timing edges. The total number of coincident pairs {totp(C)} is counted within a preset 400 ns window τ. {totp(C)}/{dur(C)} delivers the experimental coincidence rate R_e. We use the same τ to calculate the chance rate, $R_c = R_\Theta R_\Phi \tau$. All coincidence data in sections **4** and **5** refute QM. In most cases, τ can be narrowed to calculate R_e/R_c even higher, but we fixed τ to maintain comparisons. Notice there are no out-of-time pairs in the outer parts of C (wings), which are allowed to span 2 μs. The wings are from chance. This no-wings effect is a superior measure of the unquantum effect.

Each minute, the MCS records counts accumulated from four HP 5334 Universal Counters, via GPIB to the PC. Counts accumulated over the entire experiment determine our singles rates R_Φ and R_Θ from the **inc**idents and **ref**lecteds detectors. The MCS also records Lecroy triggers and counts from my muon detector. Because coincidence events are rare, these tests require 5 to 10 hours to read to a few significant figures.

During these tests, different forms of noise interference may occur:

1) Microwave bursts from cell phones can cause wildly shaped pulses on the Lecroy scope, which scrap the test. RF filters were installed in an attempt to remove such disruptions.

2) A background coincidence rate with the source removed measured only 4 in a 48-hour test on June 10, 2026. This is in the spreadsheet calculation.

3) As shown on the MCS, at rare minutes muon counts can nearly double. In that same minute, a similar enhanced count can appear on the graph of **inc**idents clicks. Only 3 of 38 recordings show this kind of interference. From inspection, these additional counts can be ignored. We attempted to compare against published solar storm and X-ray data, but reached no conclusion. The parts for this muon detector construction were a large plastic scintillator and a PMT, both surplus and of unknown specifications.

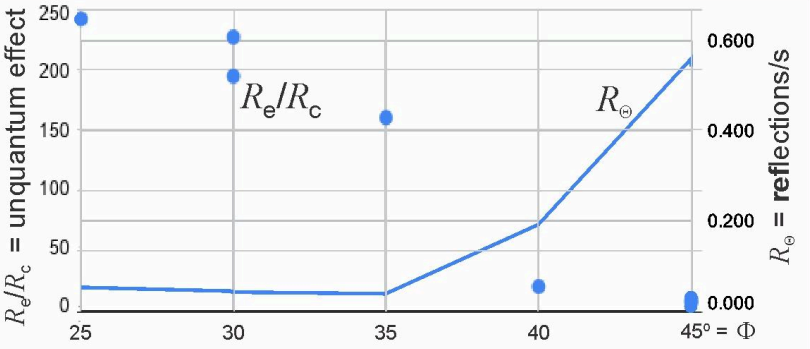


Fig. 9

R_e/R_c and R_Θ rate at ref det
Both for specular angles
$2\Phi 1 = 2\Phi 2 = \Theta$

Φ	R_e/R_c	R_Θ = reflections/s
25	242	0.050
30	194	0.042
30	227	0.040
35	160	0.036
40	20	0.190
45	7.3	0.558
45	9.3	0.542

In **Fig. 9**, we sort our tests to focus on important measures while maintaining the Bragg condition Φ1 = Φ2. The angle Θ orientation of mine and Rutherford is the same, but now with specular crystal reflection arranged with two detectors. From the viewpoint of Rutherford scattering, one might expect the α reflection rate to decline steeply with angle. In these conditions, we see a steep increase with angle. This enhancement of reflection cannot be explained by α burrowing between layers, reflecting, and being trapped on the way out, as seen in RBS. In RBS, larger angles closer to retroreflection inhibit, not enhance, reflection.

In **Fig. 9**, we also examine the unquantum effect R_e/R_c at specular angles. Under these conditions, the unquantum effect is spectacular, with a near 200-fold chance. However, a better plot can show the trend.

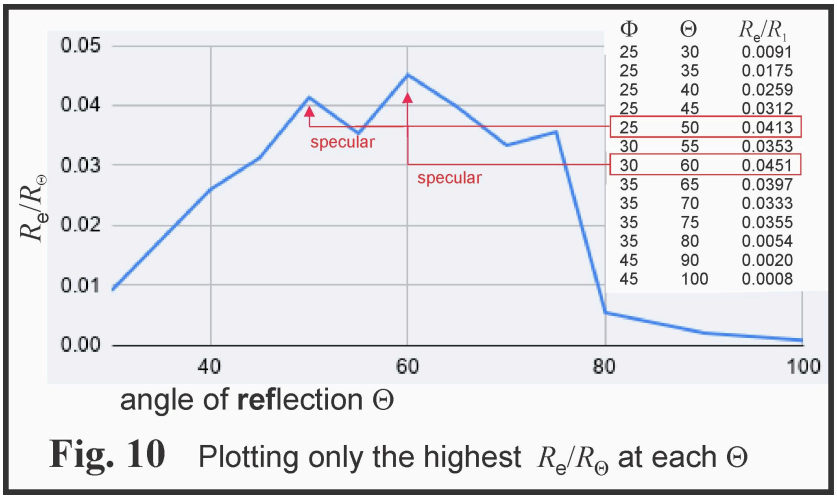


Fig. 10 Plotting only the highest R_e/R_Θ at each Θ

We now make the rate at the scattered angle R_Θ more important than the calculated chance rate and sort for R_e/R_Θ as a function of angle pairs, to find which pairs are specular (**Fig. 10**) (the other terms are constants). We now see a specular reflection at the two highest points in the graph. The peak at $2\varphi = \Theta = 60^\circ$ matches the angle in X-ray diffraction for silicon (**Fig. 11**). Although Bragg distances by X-rays are 20 thousand times larger than those by α-rays, we do not ignore this coincidence.

5) Conclusion and hypothesis

The discoveries of this report are:

1) The matter-wave unquantum effect can be enhanced with a crystalline beam splitter.

2) Upon specularly reflecting α-rays off a silicon crystal surface, the reflection rate has a trend contrary to Rutherford's theory. In the range shown in **Fig. 9**, increasing specular angles increases reflection.

3) The rate (specular coincidence rate)/(rate of reflection) peaks at specular angles 30°, consistent with Bragg reflection.

For a different collision phenomenon, the Compton effect, we discovered a beautiful symmetry. Assumptions in a particle model and different assumptions in a wave model can lead to the same equation (16, 17). Here, we explore physical evidence suggesting a similar symmetry in matter-matter collisions. A particle-oriented derivation need not prove nature is made of particles that always hold themselves together… especially in the face of nonlocality, and especially in the face of a demonstrable unquantum effect.

The unquantum effect R_e/R_c is like a filter. A matter wave can be emitted with arbitrary polarization, similar to the orientation of the transverse electric field of polarized light. Three points define a plane: source, detector 1, detector 2. We model a burst of spontaneously emitted matter waves polarized normal to the three-point plane as more likely to undergo a wave split by Bragg diffraction.

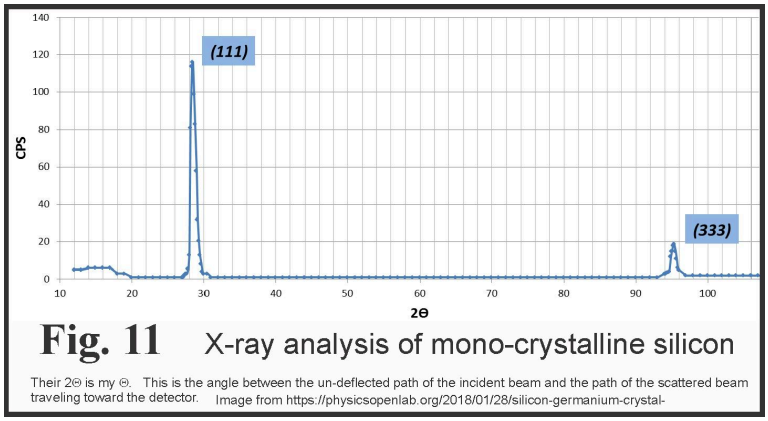


Fig. 11 X-ray analysis of mono-crystalline silicon

Their 2Θ is my Θ. This is the angle between the un-deflected path of the incident beam and the path of the scattered beam traveling toward the detector. Image from https://physicsopenlab.org/2018/01/28/silicon-germanium-crystal-

The particle Coulomb force model does not account for a scatterer's surface orientation or its crystalline state. In addition to the work in section **5**, we mention discoveries from my early γ-ray unquantum tests. R_e/R_c varied as: 1) amorphous vs crystalline state of the ^{109}Cd source (ref. 12, see *its Fig. 11*), and 2) crystal silicon beam-splitter orientation (ref. 12, see *its Fig. 13*). The γ wavelength is far too short for conventional crystallography. We explain those chemical/nuclear effects by a jump in

distance scale. I model this large jump in distance scale in my derivation of the photoelectric effect (12, 16, 17). The derivation has an electromagnetic wavelength that fits a matter-wave beat envelope composed of a higher-frequency inner wave. Here, the similarity of the X-ray Bragg diffraction angle in silicon in **Fig. 11** to the peak angle in **Fig. 10** also suggests a jump in distance scale. We model the ratio of beat wavelength to inner-wave wavelength in explaining jumps in distance scale for the two mentioned cases: 1) from light to charge, and 2) from atomic to nuclear spatial periodicities.

My experiments are slow. However, we can take advantage of time. Stronger radioisotopes can make my technique practical. This study obviously needs more work. Links to spreadsheets and all ER works are at http://www.thresholdmodel.com.

References

1. *Atom Interferometry*, Berman PR (1996).
2. Towards Realization of an Atomic de Broglie Microscope: Helium Atom Focusing Using Fresnel Zone Plates, Doak RB et al, Phys. Rev. Lett. 83, 4229 (1999).
3. On the structure of the atom: an investigation of the stability and periods of oscillation of a number of corpuscles arranged at equal intervals around the circumference of a circle; with application of the results to the theory of atomic structure, Thomson JJ, Phil Mag Ser 6. 7:237–265 (1904).
4. The Laws of Deflexion of α Particles Through Large Angles, Geiger H, Marsden E, Phil Mag 25, pages 604–623 (1913).
5. The scattering of α and β particles by matter and the structure of the atom, Rutherford E, Philosophical Magazine, Vol. 21, No. 125, pp. 669–688 (1911).
6. On the constitution of atoms and molecules, Bohr N, Philosophical Magazine, series 6 (1913).
7. *Experiments in Modern Physics*, Melissinose AC, page 231.
8. A novel design of Rutherford scattering apparatus, Eaton TW, Cheetham D, Phys Educ 8 page 97 (1973).
9. *The Atomic Nucleus*, Evans RD, Page 18 (1955)
10. Modified version of the MIT Rutherford scattering apparatus for use in advanced undergraduate laboratories, Earl JA, American Journal of Physics, Volume 34, Issue 6, pp. 483-488 (1966).
11. Backscatter anomaly in scattering of α-particles from ^{28}Si at low energies, Coban A et al, Nuclear Physics A, 678 pgs 3-10 (2000).
12. Photon violation spectroscopy (edited), Reiter ES, US patent application filed 2005 US20050139776A1 -
13. Particle Violation Spectroscopy (edited), Reiter ES, US patent application filed 2008, US20080173825
14. Backangle anomaly in scattering of alpha-particles from ^{28}Si at low energies, Coban et al, Nuclear Physics A, 678 (2000).
15. The Reflection of Atoms from Crystals, Ellett A, Olson HF, Zahl AH, PR 34, page 493 (1929).
16. New experiments call for a continuous absorption alternative to quantum mechanics-the unquantum effect, Reiter ES, Progress In Physics, vol 2 pg 82 (2014).
17. Overcoming the quantum mechanics measurement problem by experiment and theory, Reiter ES, Physics Essays, Volume 35: Pages 197-201 (2022).

Acknowledgments Ken Kitlas and Michael Kan helped with earlier alpha and gamma tests. Michael Koller crafted the title.

Appendix 1 Spreadsheet for June 2026 repeat of 1913 test

	A	B	C	D	E	F	G	H	I	J	K	L	M	N	O
1															
2		angle scat det	Gold angle	0.5 Roi:	Rbigs	roi minus backs	big minus backs	1/(sinRad(D)^4	roi/sin^4	I/G rescale	roi error I/K	big/sin^4	I/H correction	bigs error	
3				0		#	#	1/sin4 theory	G# / theory	90.00005813	should/got	H# / theory	202.986027	should / got	
4		45.00	30	22.5	0.208	0.46726	0.207174	42.05	19.64989438	42.05	1	8.712376719	42.05342716	1	
5		60.00	30	30	0.047	0.12426	0.046174	13.32	1.654801255	11.18	1.190804188	0.614910616	9.372676812	1.420858568	
6		60.00	45	30	0.039	0.11326	0.038174	13.32	1.508311526	10.19	1.306457075	0.508372631	7.748788596	1.718623239	
7		75.00	30	37.5	0.0141	0.03826	0.013274	5.48	0.209676229	3.44	1.591540542	0.072745691 26	2.694436523	2.033937039	
8	no Au roi	90.00	30	45	0.004	0.01486	0.003174	2.69	0.040011986 11	1.34	2.013305595	0.008546301743	0.644277649 8	4.179248874	
9	no Au big	90.00			0.005										
10	no Am roi			0.0026											
11	noAm big			0.00014	0.00326										
12	back sums			0.00274	0.000826										

A — no Au roi = $R_{noAuRoi}$ = background rate in Region Of Interest with gold removed
no Au big = $R_{noAuBig}$ = background rate in big-pulses spectrum with gold removed
no Am roi = $R_{noAmRoi}$ = background rate in ROI spectrum with Americium-241 removed
no Am big = $R_{noAmBig}$ = background rate in big-pulses spectrum with Americium removed
back sums = $R_{backsxx}$ = background rate with Au and ^{241}Am removed. Stated aside for Roi, Big.

B — Angle of scatterer detector

C — Angle of gold scatterer

D — Scale and offset adjustment of angle

E — Count **R**ate in **R**egion **O**f **I**nterest spectrum. R_{roi}

F — Count **R**ate in **Bigs** spectrum. R_{Bigs}

G — $R_{roi} - R_{NoAmRoi} - R_{noAuRoi}$

H — $R_{big} - R_{NoAmBig} - R_{noAuBig}$

I — Equation developed by Rutherford for rate as function of angle. "1/sin^4".

J — R_{roi}/"sin^4"

K — normalization calculation, "1/sin^4"/$R_{roi\ at\ 45^o}$.

L — Error calculation using ROI data.

M — R_{big}/"sin^4"

N — normalization calculation, "1/sin^4"/$R_{big\ at\ 45^o}$.

O — Error calculation using Bigs data.

Appendix 2 Spreadsheet for June 2026 alpha-ray against silicon detector

date 2026	phi_incidents	theta_reflects	Re/Rchance	Rexperiment	Rtheta	Rphi	Re/Rtheta	hours/chance	MCS time	reflects	Incidents	DSO secs	DSO coinc	triggers	note	Big incs	out of time DSO	Background 2/day
month/day	degrees	degrees	Unquantum	coinc/s	refls	inc/s	coincs/reflects	1/R1*R2*400ns*	seconds	# MCS	# MCS	seconds	# in window	# DSO				#/sec Use for all
05/22	25	30	52.8	0.00119	0.133	421.760	0.0089	12.3421928345640	27000	3602	11387516	25582	31	32		5	0	2.32E-05
05/21	25	35	103.8	0.00183	0.105	421.633	0.0175	15.7188653158220	30120	3156	12699577	29449	54	53	many		1	2.32E-05
05/20	25	40	151.6	0.00183	0.071	427.322	0.0259	23.0142063758800	37500	2648	16024558	37706	69	68	bigs 32xchance	16	1	2.32E-05
05/20	25	45	185.3	0.00179	0.057	421.556	0.0312	28.7343732697810	34380	1971	14493087	34615	62	61	interesting	6	0	2.32E-05
05/19	25	50	241.7	0.00208	0.050	427.309	0.0413	32.2129800418540	28860	1456	12332124	28308	59	59	best	6	0	2.32E-05
06/03	25	60	220.4	0.00151	0.040	429.912	0.0379	40.4716841942540	18240	728	7841597	16525	25	26		3	1	2.32E-05
05/19	25	65	181.2	0.00126	0.041	427.387	0.0310	39.7990045136440	37500	1531	16027015	40326	51	47	dso longer time	2	1	2.32E-05
06/01	25	70	191.1	0.00120	0.037	421.565	0.0322	44.1872151561800	37500	1398	15808703	36619	44	41	dso longer time		0	2.32E-05
06/03	25	60	220.4	0.00151	0.040	429.912	0.0379	40.4716841942540	18240	728	7841597	16525	25	26		3	1	2.32E-05
06/04	25	55	185.6	0.00137	0.044	422.167	0.0313	37.6562170886640	26280	1148	11094549	24840	34	34	peakey	5	0	2.32E-05
06/03	30	40	117.9	0.00168	0.072	495.432	0.0234	19.4753158957300	28080	2021	13911722	27345	46	49			3	2.32E-05
05/27	30	55	176.6	0.00154	0.044	499.851	0.0353	31.7585443688500	29580	1294	14786501	29140	45	46		5	2	2.32E-05
05/27	30	60	194.3	0.00163	0.042	500.690	0.0389	33.0652056355000	37500	1573	18775871	42883	70	58	dso longer time	5	0	2.32E-05
05/23	30	60	226.8	0.00180	0.040	497.201	0.0451	35.0042189398000	28320	1130	14080730	26675	48	49			3	2.32E-05
05/27	30	65	163.8	0.00124	0.038	499.968	0.0328	36.8057397256140	25200	951	12599187	24264	30	30		4	0	2.32E-05
06/04	30	50	186.0	0.00187	0.051	495.918	0.0369	27.6908378778140	28080	1420	13925387	27871	52	52	beauty peak	5	0	2.32E-05
06/05	30	70	166.5	0.00114	0.035	495.245	0.0330	40.5452469976330	29580	1023	14649347	25421	29	29	peakey		0	2.32E-05
05/28	35	55	103.1	0.00111	0.052	519.191	0.0214	25.7097028094700	36540	1901	18971227	40403	45	46	bigs 20xchance	all both at1/2 hts 9	1	2.32E-05
06/04	35	60	205.2	0.00169	0.040	517.481	0.0425	33.6947212377780	26840	1061	13786696	25421	43	44		5	1	2.32E-05
05/28	35	60	157.3	0.00125	0.038	519.139	0.0327	34.8205398309810	32460	1247	16851268	31088	39	39		2	1	2.32E-05
06/01	35	65	159.0	0.00124	0.038	518.067	0.0329	35.5133243318100	30600	1155	15852839	28946	36	37			2	2.32E-05
05/29	35	65	191.4	0.00143	0.036	518.884	0.0397	37.1603319817880	15660	564	8125729	36349	52	28	dso longer time	2	1	2.32E-05
05/29	35	70	160.0	0.00121	0.036	520.329	0.0333	36.8267879076110	26600	964	13840759	24860	30	30		2	0	2.32E-05
05/31	35	75	107.9	0.00136	0.060	519.198	0.0224	22.1153109015260	37500	2268	19469910	43517	59	34	dso longer time		4	2.32E-05
05/24	35	75	170.9	0.00131	0.037	519.741	0.0355	36.1247951105430	37500	1387	19490285	37279	49	48		1	4	2.32E-05
05/31	35	80	25.9	0.00094	0.174	518.557	0.0054	7.6945650545190	25080	4365	13005416	23520	22	26			4	2.32E-05
06/04	35	60	206.4	0.00169	0.040	514.478	0.0425	33.8913969628040	26640	1061	13706696	25421	43	44		5	1	2.32E-05
06/01	40	50	107.7	0.00106	0.047	528.421	0.0227	28.3141344326760	23760	1107	12507758	21762	23	24		3	1	2.32E-05
05/24	40	75	88.3	0.00110	0.059	528.769	0.0186	22.4072353545340	27960	1645	14728471	36529	40	40	all in time	0	0	2.32E-05
05/25	40	80	20.4	0.00082	0.190	528.822	0.0043	6.9348454395430	37500	7128	19755843	39096	32	35	interesting	4	4	2.32E-05
06/05	40	60	129.0	0.00104	0.038	528.405	0.0272	34.6192103964660	25140	958	13233825	22221	23	24		1	1	2.32E-05
06/02	45	45	19.4	0.00017	0.042	530.298	0.0041	31.2598767602530	26640	1116	14127148	23223	4	4	maybe shadow		0	2.32E-05
06/02	45	50	55.9	0.00049	0.041	530.411	0.0119	31.8468007043700	25200	1036	13366356	22555	11	11		3	0	2.32E-05
06/02	45	90	7.3	0.00086	0.558	530.052	0.0015	2.3461596594410	22920	12799	12148793	19676	17	28			11	2.32E-05
05/26	45	90	9.3	0.00107	0.542	530.422	0.0020	2.4165033243775	37500	20317	19890838	44018	47	60	dso longer time	many		2.32E-05
06/03	45	100	3.5	0.00082	1.087	538.874	0.0008	1.1857990494230	28200	30647	15196258	28111	23	43			10	2.32E-05

Φ angle of **inc**idents detector

Θ angle of **ref**lecteds detector

unquantum effect = R_e/R_c,
where R_c = chance = $R_\Theta R_\Phi \tau$

R_e= Experimental coincidence rate within τ window

R_Θ= reflections/second

R_Φ= incident counts/second

R_e/R_Θ

$1/R_c$ in hours. # of hours to expect a chance coinc.

Time of experiment recorded on MCS

R_Θ rate of reflection clicks recorded from MCS

R_Φ rate of incident clicks recorded from MCS

time duration of experiment from Lecroy scope

R_e coincidenc counts within τ from Lecroy scope.
τ = 400 ns.

trigger counts from Lecroy recorded on MCS

# of pulses > 3v from **inc**idents detector.

triggered pulses outside τ window
but in trigger window

background coincidences, source removed.
To be subtracted from R_e

Appendix 3 Photo of alpha lab

